The SDSS High Latitude Cloud Survey

Peregrine M. McGehee[1]

ABSTRACT

The high latitude clouds ($|b| > 30$) are primarily translucent molecular clouds and diffuse Galactic cirrus with the majority of them seen at high latitude simply due to their proximity to the Sun. The rare exceptions are those, like the Draco and other intermediate or high velocity clouds, found significantly above or below the Galactic plane. To date, star formation has only been verified in MBM 12 and MBM 20, which are two of the densest high latitude molecular clouds.

We present results from an ongoing study of high latitude clouds based on the Sloan Digital Sky Survey (SDSS) and the Two Micron All-Sky Survey (2MASS). This study consists of two major efforts, the first (described here) to provide a 3-D mapping of the interstellar dust using a color-excess technique, the second to identify candidate low-mass Classical T Tauri stars in the field.

Subject headings: ISM: dust, extinction — ISM: structure

1. Introduction

The spatial distribution of interstellar clouds at high Galactic latitude remains largely unknown as witnessed by the paucity of distances in the recent compendium by Dutra & Bica (2002). Cloud distances have been determined by techniques such as comparison of off-cloud and on-cloud star counts, bracketing of cloud location by the detection of absorption features in the spectra of early type stars, and by statistical estimates based on an assumed dust scale height above the galactic plane. In this paper we present a technique based on determining the reddening of stellar colors with distance and apply it to map the interstellar clouds found within the Sixth Data Release (DR6) of the SDSS.

The foundations of this color excess technique are the extinction-distance diagrams of Neckel & Klare (1980) with representative applications including the distance determination

[1]Infrared Processing and Analysis Center, MS 220-6, Caltech, Pasadena, CA 91125

of 25 high latitude clouds by Penprase (1992) and the studies of the Bok globule CB 107 and CB 24 by Strafella et al. (2001) and Peterson & Clemens (1998). In common with Peterson & Clemens (1998) we use M dwarfs as the tracers for interstellar extinction, with our motivations being two-fold. First, due to the work of Hawley et al. (2002), West, Walkowicz & Hawley (2005), and Jurić et al. (2008) we understand the stellar color-absolute magnitude relations in the SDSS passbands. We utilize reddening-invariant colors and absolute magnitudes based on these relations to compute photometric distance moduli. Secondly, the relatively high abundance of M stars allows investigation of small regions on the sky. Our analysis technique differs from that of Peterson & Clemens (1998) in that while they analyze stars individually using a Monte Carlo technique for error estimation we compute the mean and standard error in $E(B-V)$ based on the M dwarf $g-z$ color excess within three-dimensional bins spanning 2-D patches on the sky and along the line-of-sight distance.

2. Observations

The SDSS obtains deep photometry with asinh magnitude (Lupton, Gunn, & Szalay 1999) limits (defined by 95% detection repeatability for point sources) of $u = 22.0$, $g = 22.2$, $r = 22.2$, $i = 21.2$ and $z = 20.5$. These five passbands, *ugriz*, have effective wavelengths of 3540, 4760, 6290, 7690, and 9250 Å, respectively. A technical summary of the SDSS is given by York et al. (2000). The SDSS imaging camera and telescope are described by Gunn et al. (1998) and Gunn et al. (2006), respectively. Ivezić et al. (2004) discuss the data management and photometric quality assessment system.

The Data Release Six (DR6) is presented by Adelman-McCarthy et al. (2008). Pier et al. (2003) describe the astrometric calibration of the survey and the network of primary photometric standard stars is described by Smith et al. (2002). The photometric system itself is defined by Fukugita et al. (1996), and the system which monitors the site photometricity by Hogg et al. (2001); Tucker et al. (2006). Abazajian et al. (2003) discuss the differences between the native SDSS 2.5m *ugriz* system and the $u'g'r'i'z'$ standard star system defined on the USNO 1.0m (Smith et al. 2002). The Schlegel, Finkbeiner, & Davis (1998) FIR-derived $E(B-V)$ map covering the DR6 survey area is shown in Figure 1.

3. Technique

The nearest high latitude molecular clouds, e.g. MBM 7, MBM 16, MBM 18, are within 100 pc ($m - M = 5$). In order to map similar nearby structures the SDSS saturation limits

of $m \sim 14$ to 15 in all bands mandate use of stars whose absolute magnitudes are fainter than 10. From West, Walkowicz & Hawley (2005) we see that this condition is fulfilled by low-mass stars with spectral types later than M3.

The use of M dwarfs as extinction probes rules out reliance on the SDSS u band for two reasons even though this band is the most sensitive to the presence of extinction. First, the extreme faintness of M dwarfs in this band ($u - g \sim 2.5$) limits the distance that interstellar dust structures can be surveyed. The second reason is the presence of a u-band red leak in the SDSS imager. This detector effect has a value, albeit with a significant dispersion, of approximately 0.1 to 0.3 magnitudes for early to mid M dwarfs (Abazajian et al. 2004)

The calibration between a reddening-invariant index formed from the SDSS $griz$ bands and the intrinsic $g - z$ color is obtained using the median stellar locus of Covey et al. (2007). The effective dispersion in this relation is studied using stars along sightlines have minimal SFD98 reddening. The mean of the "faint" and "bright" normalized photometric parallaxes from Jurić et al. (2008) is used to assign distances to specific stars. The issues of sample contamination by background giants, white dwarf-M dwarf binaries, and low metallicity subdwarfs are considered and a statistical correction is made to derived distances based on the relative occurrence of binarity.

4. Maps

We generate maps of each target dust cloud by first applying a local gnomonic (tangent plane) projection. We define patches in Equatorial coordinates on this local map and compute the mean and standard error in $E(B - V)$ in a series of distance bins. The S/N ratio of each detection is defined as the ratio of the mean to the standard error.

4.1. Test Cases

In order to assess the performance of this method we use three well-studied regions as test cases. These regions are the high latitude cloud MBM 12, the Orion OB1 association, and the Taurus star formation region. SDSS imaging of the latter two areas forms part of the low-latitude or "Orion" data release (Finkbeiner et al. 2004).

- **MBM 12.** The high latitude molecular cloud MBM 12 is an extensively studied local star formation region. MBM 12 is a suitable test case due to its relative isolation, its opacity (it is associated with several Lynds dark nebulae), and reliable distance

estimates.

We generated a local map centered at $(\alpha_{2000}, \delta_{2000})$=(44.21,+19.53) and selected an on-cloud (center=(0.0, 0.0), boxsize=0.5, "A") and an off-cloud (center=(1.0,0.0), boxsize=0.5, "B") patch. The distance bin used in each patch is 50 pc. The on-cloud reddening profile (Figure 2) shows a cloud location consistent with the 360±30 pc value obtained by Andersson et al. (2002).

- **Taurus.** The distance to the Taurus star formation region is well-determined with the standard value given as 140 pc. Due to the saturation limit of the SDSS imaging this cloud is close to minimum detection limit for this survey. We study a single 0.5 by 0.5 degree patch centered at $(\alpha_{2000}, \delta_{2000})$=(65.00,+25.00) using a 50 pc bin size. The Taurus cloud is clearly detected (Figure 3) with stars in the 50-100 pc and 100-150 pc bins having reduced reddening as expected for foreground objects.

- **Orion**. For the Orion equatorial region we study three patches on a field centered at $(\alpha_{2000}, \delta_{2000})$=(88.00,+0.00). These span 0.5 by 0.5 degrees and are centered at (-1.0,0.0), (0.0,0.0), and (1.0,0.0) for patches "A","B", and "C", respectively. Patches "B" and "C" show reddening profiles consistent with the distance of 440 pc to the Orion OB1b association and molecular cloud (Figure 4). The profile for patch "A" is complicated by the presence of pre-main-sequence stars in the NGC 2268 protocluster as young stars are more intrinsically luminous and often possess significant local extinction due to circumstellar material.

5. Summary

We have demonstrated that analysis of SDSS photometry of M dwarfs can be used to probe dust structures in the local ISM within 1 kpc. This will be used to assign distances to high latitude clouds to study their distribution and properties. In addition, knowing the distance to these potential stellar nurseries will enable characterization of any associated stellar populations.

Funding for the SDSS and SDSS-II has been provided by the Alfred P. Sloan Foundation, the Participating Institutions, the National Science Foundation, the U.S. Department of Energy, the National Aeronautics and Space Administration, the Japanese Monbukagakusho, the Max Planck Society, and the Higher Education Funding Council for England. The SDSS Web Site is http://www.sdss.org/.

The SDSS is managed by the Astrophysical Research Consortium for the Participating Institutions. The Participating Institutions are the American Museum of Natural History, Astrophysical Institute Potsdam, University of Basel, University of Cambridge, Case Western Reserve University, University of Chicago, Drexel University, Fermilab, the Institute for Advanced Study, the Japan Participation Group, Johns Hopkins University, the Joint Institute for Nuclear Astrophysics, the Kavli Institute for Particle Astrophysics and Cosmology, the Korean Scientist Group, the Chinese Academy of Sciences (LAMOST), Los Alamos National Laboratory, the Max-Planck-Institute for Astronomy (MPIA), the Max-Planck-Institute for Astrophysics (MPA), New Mexico State University, Ohio State University, University of Pittsburgh, University of Portsmouth, Princeton University, the United States Naval Observatory, and the University of Washington.

Facilities: SDSS.

REFERENCES

Abazajian, K., et al. 2003, AJ, 126, 2081

Abazajian, K., et al. 2004, AJ, 128, 502

Adelman-McCarthy, J. K., et al. 2008, ApJS, 175, in press (Data Release 6)

Andersson, B.-G., Idzi, R., Uomoto, A., Wannier, P. G., Chen, B., & Jorgensen, A. M. 2002, AJ, 124, 2164

Covey, K. R., et al. 2007, AJ, 134, 2398

Dutra, C.M. & Bica, E. 2002, A&A, 383, 631

Finkbeiner, D. P., et al. 2004, AJ, 128, 2577

Fukugita, M., Ichikawa, T., Gunn, J.E., Doi, M., Shimasaku, K., & Schneider, D.P. 1996, AJ, 111, 1748

Gunn, J.E. et al 1998, AJ, 116, 3040

Gunn, J.E. et al. 2006, AJ, 131, 2332.

Hawley, S.L. et al. 2002, AJ, 123, 3409

Hogg, D.W., Finkbeiner, D.P., Schlegel, D.J., & Gunn, J.E. 2001, AJ, 122, 2129

Ivezić, Ž, Lupton, R.H., Schlegel, D. et al. 2004, AN, 325, No. 6-8, 583-9.

Jurić, M., et al. 2008, ApJ, 673, 864

Lupton, R.H., Gunn, J.E., & Szalay, A.S. 1999, AJ, 118, 1406

Neckel, Th. & Klare, G. 1980, A&A, 42. 251

Penprase, B.E. 1992, ApJS, 83, 273

Peterson, D. & Clemens, D. 1998, AJ, 116, 881

Pier, J.R., Munn, J.A., Hindsley, R.B., Hennessy, G.S., Kent, S.M., Lupton, R.H., & Ivezic, Z. 2003, AJ, 125, 1559

Schlegel, D., Finkbeiner, D. & Davis, M. 1998, ApJ, 500, 525

Smith, J.A. et al 2002, AJ, 123, 2121

Strafella, F. et al 2001, ApJ, 558, 717

Tucker, D. L, et al. 2006, AN, 327, 821

West, A.A., Walkowicz, L.M., & Hawley, S.L. 2005, PASP, 117, 706

York, D. et al. 2000, AJ, 120, 1579

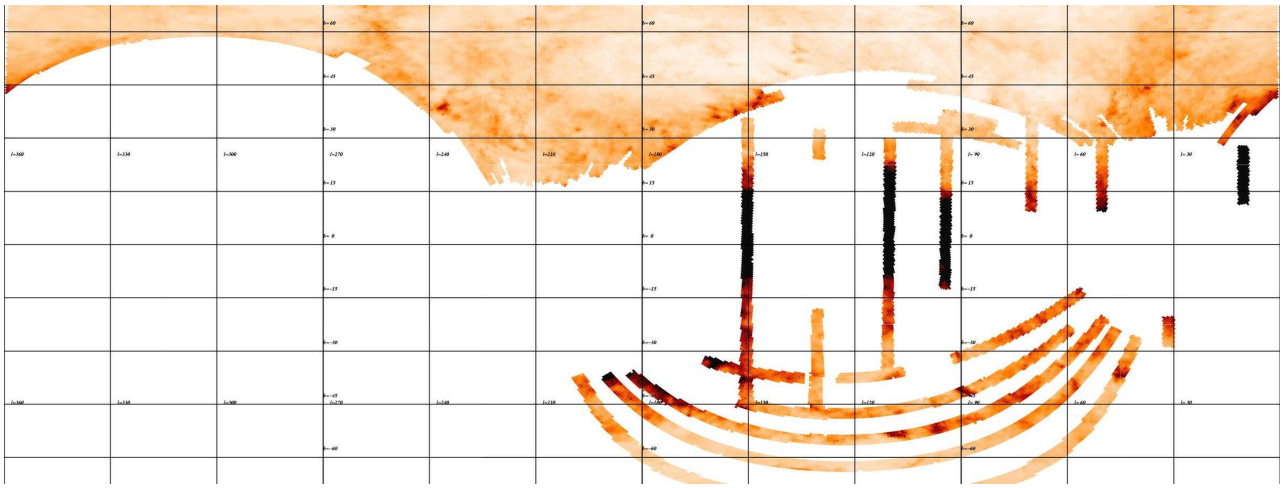

Fig. 1.— **SDSS DR6 survey area.** The variation of the FIR-derived interstellar reddening (Schlegel, Finkbeiner, & Davis 1998) with Galactic longitude and latitude is shown here for the SDSS Data Release 6 imaging footprint.

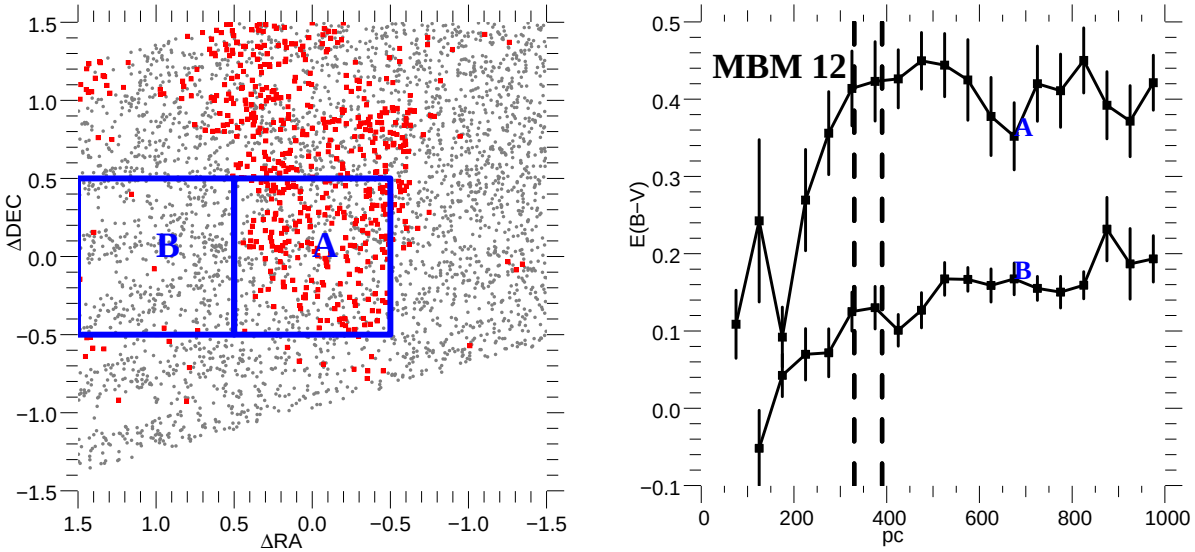

Fig. 2.— **MBM 12 Test Case.** The distribution of stars in the MBM 12 field is shown in the left hand panel. The on and off cloud regions ("A" and "B", respectively) are indicated and stars with computed $E(B-V)$ values greater than the average of the SFD98 values for the field are highlighted in red. The right hand panel shows the mean and standard error in computed $E(B-V)$ for both patches. The dashed lines mark the 330-390 pc distance determined by Andersson et al. (2002).

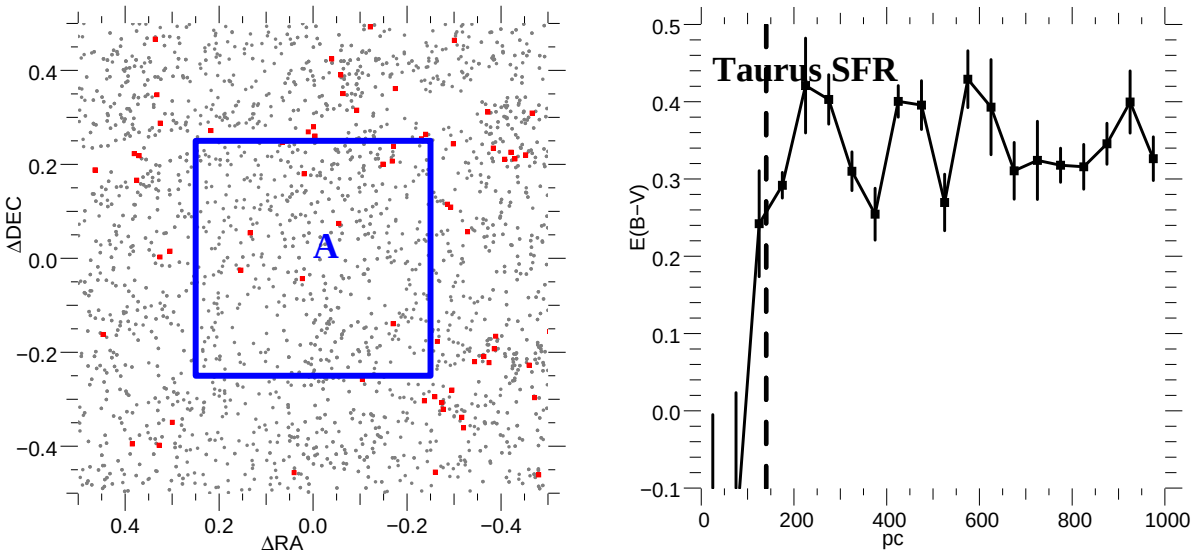

Fig. 3.— **Taurus Test Case.** The distribution of stars in the Taurus field is shown in the left hand panel. The study region ("A") are indicated and stars with computed $E(B-V)$ values greater than the average of the SFD98 values for the field are highlighted in red. The right hand panel shows the mean and standard error in computed $E(B-V)$ versus distance. The dashed line marks the 140 pc distance.

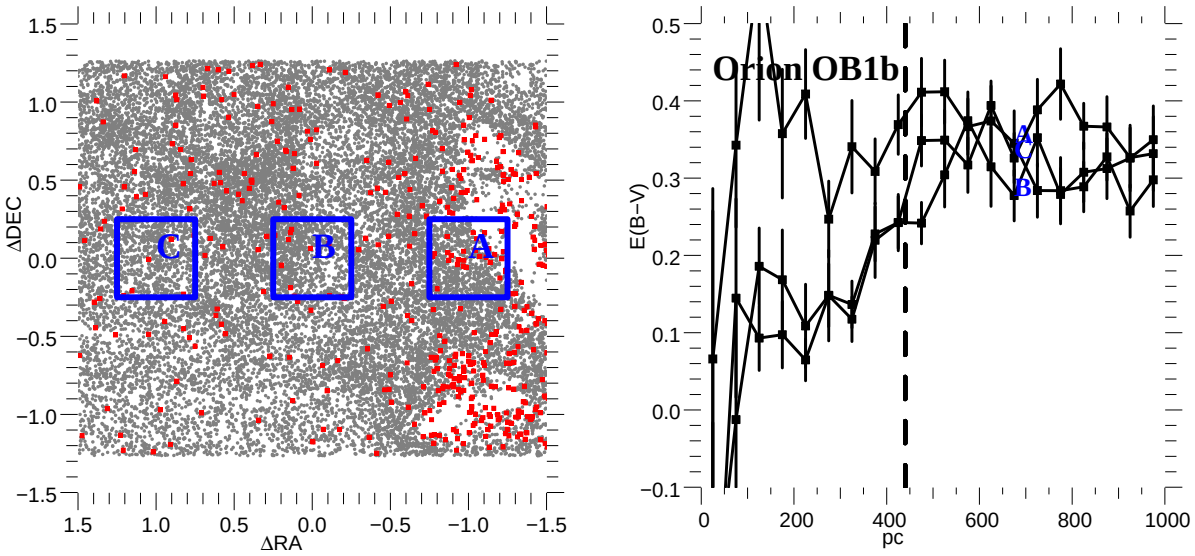

Fig. 4.— **Orion Test Case.** The distribution of stars in the Orion equatorial field is shown in the left hand panel. The three study regions ("A", "B", and "C") are indicated. The reddening is overestimated for apparently nearby stars in patch "A" due to dominance of the pre-main sequence population. The dashed lines mark the 440 pc distance to the Orion OB1b assocation and molecular cloud.